

# A Novel Forward Approach Method for the Converted Electric Car with Modeling and Performance

Satuluri Likitha Naga Vigneswari<sup>1</sup>, Jonnadula Venkata Rahul<sup>1</sup>, Kommalapati Siddhardha<sup>1</sup>, Ravipati Sindhu Priya<sup>1</sup>, Damarla Bhuvan Sri Sai<sup>1</sup>, Kommuri Vijay Manikanta<sup>1</sup>

<sup>1</sup>School of Computer Science and Engineering, VIT-AP University, G-30, Inavolu, Beside AP Secretariat Amaravati, Andhra Pradesh 522237

\*\*\*

**Abstract** - Electric vehicles show promising results to lower carbon emissions in the world. However, electric vehicles are comparatively costly and have an issue of range anxiety. Electric vehicle conversion acts as a transition state before full electrification can be achieved in the automobile industry. In this paper, a MATLAB Simulink model is developed to estimate the total energy consumption and range of an electric converted safari vehicle. The model is used to select desired vehicle parameters like electric motor power and optimum gear ratio for desired top speed. Different blocks of the Forward Approach Model: longitudinal vehicle dynamics, powertrain system, battery model, and driver model are integrated with non-linear and dynamic characteristics, which resulted in accurate estimation of driving parameters. The results showed a 36% error in estimating starting motor torque which indicates that the converted vehicle had a lower gear ratio than the simulated model and unaccounted losses were not present in the simulated model. Similarly, the results showed a 1% fluctuation in SOC of the battery due to the intricacies involved in simulating the exact behavior of the provided battery.

**Key words:** Electric vehicle, Electric Conversion Process, Forward Approach method, MATLAB Simulink,

## 1. INTRODUCTION

In the context of Nepal, the share of fossil fuel vehicles is on the rise. From 1990-2011, vehicles in the country have increased at an average growth rate of 14.32% [1]. With almost all of the vehicles running on petroleum fuels, only a modicum portion comprises of an electric vehicle. Nearly 76% of imported fuel energy is used for road transportation purpose. For the last 10 years, the importing trend of petroleum products is increasing at an average growth rate of 12.08%, as per the 2019/20 report of Nepal Oil Corporation. Moreover, the burning of fossil fuels is the primary cause of climate change, altering the Earth's ecosystems and causing human and environmental health problems. In 2020, the CO<sub>2</sub> emission per capita for Nepal was 0.59 tons of CO<sub>2</sub> per capita. CO<sub>2</sub> emission per capita of Nepal increased from 0.02 tons of CO<sub>2</sub> per capita in 1971 to 0.59 tons of CO<sub>2</sub> per capita in 2020 growing at

an average annual rate of 8.18% [2]. Based on these facts, electrification of the transportation sector is imperative to tackle global warming and economic import-export imbalance problems in developing countries like Nepal. Considering the financial curb and the available choices of new vehicles, vehicle conversion becomes an effective investment alternative in line with vehicle utility purposes. The capital investment needed to convert an old petroleum-fueled vehicle into an EV of a specific performance is comparatively cheaper than buying a new EV of the same performance [3].

In Nepal, the regulation to run converted EVs on public roads is still in its embryonic stage. Therefore, this research targeted converting petroleum-fueled vehicles into EVs inside Chitwan National Park, Nepal. A safari vehicle was selected to be converted to Battery Electric Vehicle (BEV) as a prototype to test the simulation results. The model-based design process was adopted for EV conversion development. The process is used to perform system simulations based on different scenarios and technical specifications. The method benefits the design engineer in making better decisions for the conversion and also saves time and cost by reducing errors during the design process. This method was used to validate design requirements and EV conversion specifications [4].

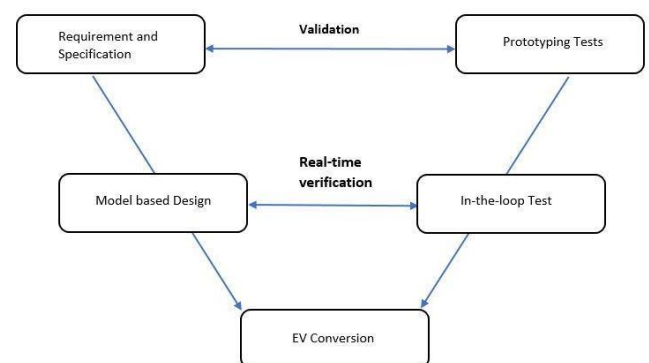


Fig-1: Model based design process

At first, analytical calculations required for model development were carried out. Using the forward

approach method, a mathematical model using MATLAB Simulink was developed. EVs are generally tested for WLTC Class 3a [5], but the model was tested with experimental data obtained through vehicle monitoring software. The cruising speed inside the national park is limited, so lower vehicle speed, like in experimental data, is viable for the simulation. The model is used to study the load capacity limit of the electric motor and the optimum gear ratio to be selected for desired top speed and acceleration. Different blocks of the forward approach model [6]; longitudinal vehicle dynamics, powertrain characteristics, regenerative braking, battery model, and driver model are integrated with non-linear and dynamic characteristics which contributed in the estimation of driving parameters. And finally, the model is applied in a prototype and the simulation and actual results were compared and discussed.

## 2. DEVELOPMENT AND ANALYSIS OF THE EV MODEL

The Simulink architecture is based on the forward modeling approach [6]. The forward model approach is an effect-cause method: the driver has to accelerate or hit the brake to reduce the error between the actual speed and the drive cycle speed, which is shown in the figure 2.

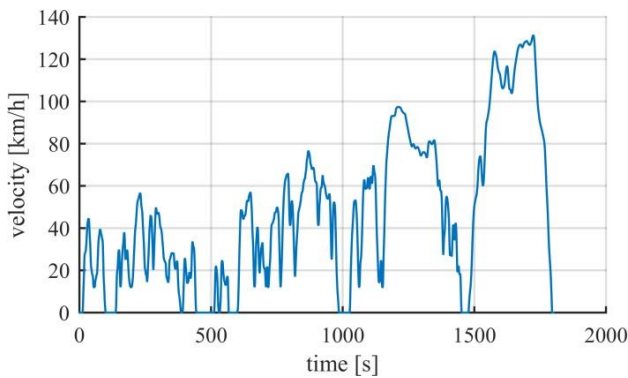


Fig-2: WLTC class 3 drive cycle graph

The vehicle system model is divided into 5 parts: Powertrain/Transmission model, Electric motor model, Vehicle dynamics model, Driver model, and Battery model. The input parameters used while developing the vehicle model in MATLAB Simulink are given below in table 1.

Table -1: Simulation parameters for the converted vehicle

Parameters	Value with units
Adhesion coefficient ( $\varphi$ )	0.85
Frontal area of vehicle ( $A_f$ )	2 m <sup>2</sup>

Density of air ( $\rho$ )	1.22 kg/m <sup>3</sup>
Coefficient of drag ( $C_d$ )	0.35
Slope angle ( $\theta$ )	0 degree
Vehicle weight ( $M_{\text{vehicle}}$ )	1400
Rotary inertia coefficient( $\delta$ )	1.15
Radius of wheel ( $R_{\text{wheel}}$ )	0.381 m
Gear ratio ( $G$ )	4.88
Transmission efficiency ( $\eta_T$ )	0.85
Motor efficiency ( $\eta_M$ )	0.97
Inverter efficiency ( $\eta_I$ )	0.98
Auxiliary power ( $P_{\text{aux}}$ )	300 W
Max torque ( $T_{\text{max}}$ )	180 Nm
Max regenerative braking power (Regen <sub>max</sub> )	3000 W
Cell nominal capacity ( $C_{\text{cell}}$ )	2.5 Ah
Number of cells ( $N_{\text{cell}}$ )	2400

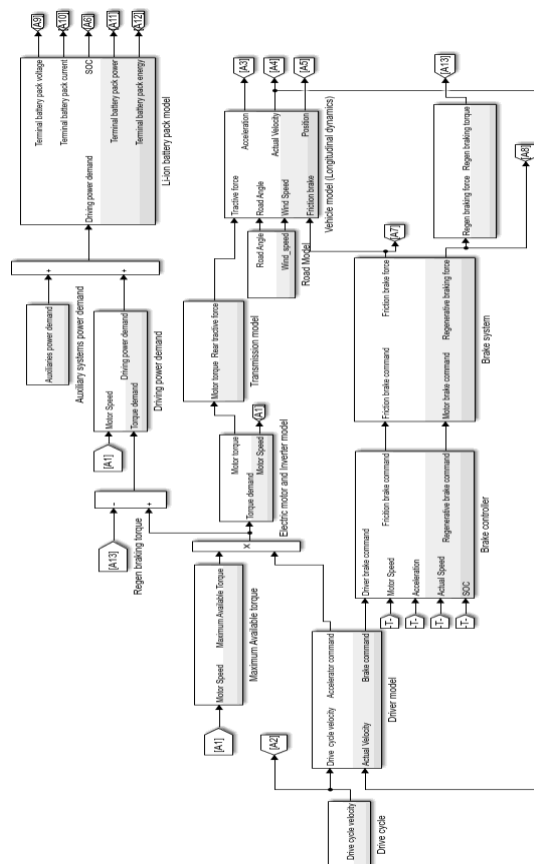


Fig-3: Simulink architecture of the proposed EV

### 2.1 Transmission Model

The converted vehicle is rear-wheel drive system in which a motor is coupled with a differential system. The torque is transferred from the motor to wheels through the transmission system. In the model, drive cycle velocity is the input, so motor rpm was calculated by using the equation:

$$\text{Motor rpm} = \text{Drive cycle Velocity} * \left( \frac{60 * G}{2 * \pi * R_{\text{wheel}}} \right) \tag{1}$$

Where, G is the final gear ratio of the vehicle and  $R_{\text{wheel}}$  is the dynamic tire radius in (m).

The tractive force was calculated from the following equation:

$$F_T = \frac{T_{\text{motor}} * G * \eta_T}{R_{\text{wheel}}} \tag{2}$$

where  $F_T$  is the tractive force in (N),  $T_{\text{motor}}$  is the torque output in (Nm) from the motor,  $\eta_T$  is the transmission efficiency of the powertrain.

### 2.2 Electric Motor Model

Torque output from the electric motor is derived from the look-up table for Torque vs Motor rpm graph provided by the manufacturer. The energy flow from a battery pack to motor output is reduced due to losses present in the Electric motor and Inverter. Electric motor and Inverter efficiencies are functions of motor speed and motor torque [7]. Since actual efficiency map was not available, a constant motor efficiency of 97% and inverter efficiency of 98% are assumed. Efficiencies in traction and regenerative mode are different, but it is assumed to be equal in the study.

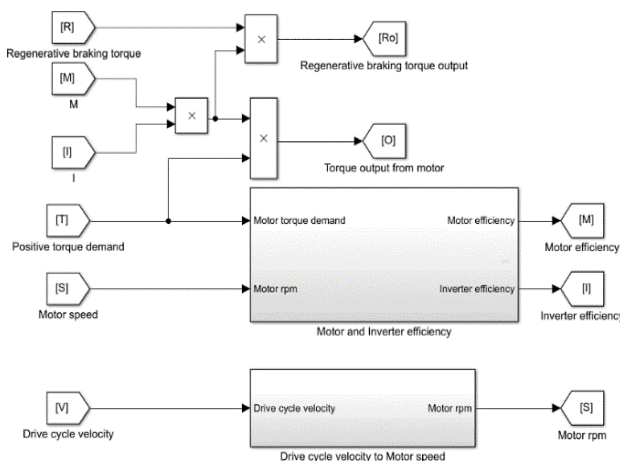


Fig-4: Electric motor model

### 2.3 Longitudinal vehicle dynamics model

During the motion of the vehicle, different resisting forces act on the vehicle [8]. Aerodynamic drag occurs due to friction created by the air around the vehicle's body as it passes by.

$$F_{\text{aero}} = 0.5 * C_d * A_f * V_{\text{vehicle}}^2 \tag{3}$$

Where,  $C_d$  is coefficient of drag,  $A_f$  is frontal area of the vehicle and  $V_{\text{vehicle}}$  is velocity of the vehicle.

Tire rolling resistance is created due to friction between tires and the road.

$$F_{rr} = C_{rr} * M_{\text{vehicle}} * g * \cos(\theta), \tag{4}$$

where  $C_{rr}$  is the coefficient of rolling resistance,  $M_{\text{vehicle}}$  is the gross weight of the vehicle,  $g$  is the acceleration due to gravity and  $\theta$  is the road slope.  $C_{rr}$  is dynamic and varies

with vehicle speed and road quality [9]. For concrete roads,  $C_{rr}$  can be approximated using equation (5) for speeds up to 128 km/h [10]:

$$C_{rr} = 0.01 * \left( 1 + \frac{V_{\text{vehicle}}}{100} \right) \tag{5}$$

Gradient resistance is caused due to component of gravity acting on the vehicle because of the road slope.

$$F_{\text{grad}} = M_{\text{vehicle}} * g * \sin(\theta) \tag{6}$$

To accelerate, the vehicle needs to overcome inertial force ( $I_L$ ) and rotary inertia of rotating parts ( $I_R$ ) in the vehicle system. Total inertial resistance ( $F_I$ ) is given by the equation:

$$F_I = I_L + I_R = M_{\text{vehicle}} * \alpha * \delta, \tag{7}$$

Where,  $\alpha$  is linear acceleration of the vehicle and  $\delta$  is coefficient of rotary inertia which is assumed to be 1.15. The rotary moment of inertia can be accurately calculated using the method mentioned in [11] [12].

The electric motor needs to overcome the resisting forces for the vehicle to accelerate, so the total tractive force ( $F_t$ ) is given by the equation:

$$F_t = F_{\text{aero}} + F_{rr} + F_{\text{grad}} + F_I \tag{8}$$

Thus, the acceleration of the vehicle is given by the equation:

$$a = \frac{F_t - F_{\text{aero}} + F_{rr} + F_{\text{grad}}}{M_{\text{vehicle}} * \delta} \tag{9}$$

## 2.4 Driver Model

A PD controller is used for the accelerator and brake commands. The controller is fine-tuned with Simulink's inbuilt tuner app for the least error between the drive cycle and actual vehicle speed.

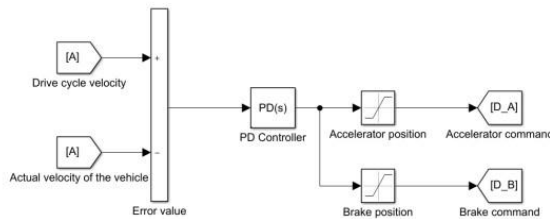


Fig-5: PD controller model

### 2.4.1 Brake Strategy Model

The braking strategy has a strong effect on both fuel economy and the performance of the converted vehicle[21]. Since the model employed a series braking system at the rear axle, the maximum available braking force ( $X_{BMAX}$ ) is distributed between friction braking force ( $X_{Friction}$ ) and regenerative braking force ( $X_{Regen}$ ) [6] [13].

$$X_{BMAX} = \varphi * M_{vehicle} * g, \tag{10}$$

Where  $\varphi$  is the adhesion coefficient between the tires and the road.

$$X_{Friction} = X_{BMAX} * D_{Friction} \tag{11}$$

$$X_{Regen} = X_{BMAX} * D_{Regen} \tag{12}$$

Where  $D_{Friction}$  is the friction braking command and  $D_{Regen}$  is the regenerative braking command.

The demanded motor braking power  $P_{Br\_demanded}$  is compared to the maximum regenerative motor braking power  $P_{Max\_Regen}$  to derive the limited motor braking torque  $T_{Br\_Limited}$ .  $P_{Br\_demanded}$  is the power required to decelerate the vehicle to a certain speed [14]. The algorithm for braking is as follows:

If  $P_{Br\_demanded} > P_{Max\_Regen}$ :

$$T_{Br\_Limited} = \frac{P_{Max\_Regen}}{\omega_{motor}}, \text{ if } \omega_{motor} \neq 0$$

$$= 0, \text{ if } \omega_{motor} = 0$$

If  $P \leq P_{Max}$  :

$$= 0, \text{ if } \omega_{motor} = 0$$

Where  $\omega_{motor}$  is the motor rpm. The available electric motor brake command ( $EM_{Available}$ ) is compared with the driver's brake command ( $D_B$ ), to calculate the friction braking force and regenerative braking force:

$$EM_{Available} = \frac{T_{Br\_Limited} * G * \eta_T}{R_{wheel} * X_{BMAX}} \tag{13}$$

If  $D_B < EM_{Available}$ :  $D_{Regen} = D_B$ ,  $D_{Friction} = 0$

If  $D_B \geq EM_{Available}$ :  $D_{Regen} = EM_{Available}$ ,  $D_{Friction} = D_B - EM_{Available}$

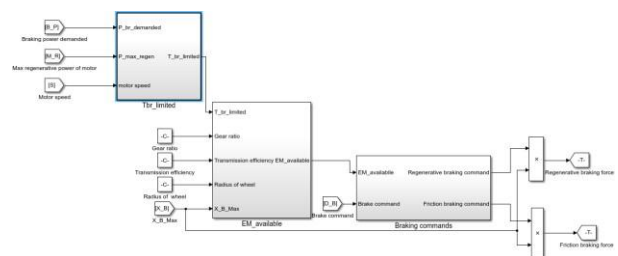


Fig-6: Braking strategy model

### 2.4.2 Torque Demand

The driver model simulates the reaction of the driver while accelerating or decelerating. The torque demand depends on the accelerator command from the driver model.

$$T_{Dem} = T_{max} * D_A \tag{14}$$

Where,  $T_{Dem}$  is the demanded torque,  $T_{max}$  is the max torque output of the motor, and  $D_A$  is the accelerator command from the driver's model.

## 2.5 Battery Model

There are different techniques to model Lithium-ion batteries: Mathematical modeling, Electrochemical modeling, and Equivalent circuit modeling [15] [16]. A generic battery model is used because the data sheets are readily available and it provides acceptable accuracy for battery parameter estimation. The components of the generic battery model include: Battery constant voltage ( $V_{oc}$ ), internal resistance ( $R_o$ ), exponential zone amplitude ( $A$ ), exponential zone time constant inverse ( $B$ ), filtered current ( $i^*$ ), current ( $i$ ), actual battery charge ( $it$ ), battery capacity ( $Q$ ) and polarization constant ( $K$ ).

$$V_{bat} = V_{oc} - K * i^* * \left( \frac{Q}{Q-it} \right) + A * \exp(-B * it) - K * \left( \frac{Q}{Q-it} \right) * i^* - R_o * i \tag{15}$$

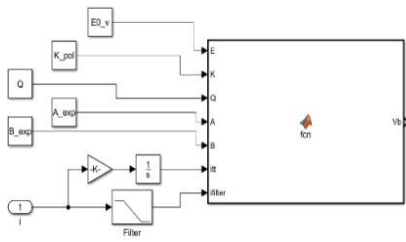


Fig-7: Generic battery model

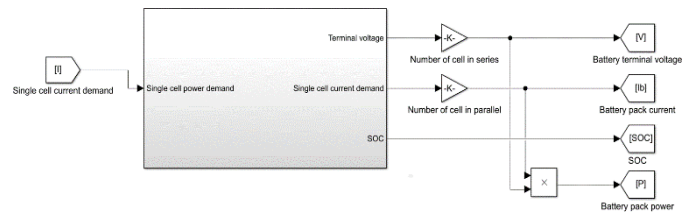


Fig-8: Battery model

Table -2: Battery parameters for Li-ion cell

Parameters	Value
Voc	3.366
R <sub>0</sub>	0.01
A	0.26422
B	26.5487
K	0.0076

Single cell current demand ( $I_{Cell}$ ) can be calculated using the equation [18]:

$$I_{cell} = \frac{(V_{OC} - \sqrt{(V_{OC}^2 - 4 * R_0 * P_{cell\_demand})})}{(2 * R_0)} \tag{16}$$

Where,  $P_{cell\_demand}$  is the single cell power demand.

Single-cell power demand is calculated by dividing the net power demand by the total number of cells ( $N_{cell}$ ).

Terminal battery pack voltage and current are given as:

$$V_{Battery\_pack} = V_1 * N_{series} \tag{17}$$

$$I_{Battery\_pack} = I_{cell} * N_{parallel} \tag{18}$$

Where,  $N_{parallel}$  is the number of cells in parallel inside the battery pack.  $N_{series}$  is the number of cells in series inside the battery pack.

The battery state of charge (SOC) is calculated using “Coulomb counting method”, given by the equation below:

$$SOC = SOC_0 - \int_0^t \frac{I_{cell}(t)}{C_{cell}} * dt \tag{19}$$

Where,  $SOC_0$  is the initial battery state of charge and  $C_{cell}$  is single cell capacity.

Lithium-ion battery pack has a stable discharge period within the state-of-charge range of 20% to 80% [20]. But, 85% of total battery energy is assumed in the study.

$$Battery_{energy} = 0.85 * Nominal_{Batt\_V} * Nominal_{Batt\_Ah} \tag{20}$$

Where,  $Nominal_{Batt\_V} = 108$  V, is the nominal battery pack voltage and  $Nominal_{Batt\_Ah} = 200$  Ah is the nominal battery pack capacity.

So,  $Battery_{energy} = 18360$  Wh

The range of the vehicle model is calculated as follows:

$$Range = \frac{Battery_{energy\ available}}{\frac{Wh}{km} \ (Value\ in\ the\ given\ drive\ cycle)} \tag{21}$$

Where,  $\frac{Wh}{km}$  value =  $\frac{Total\ energy\ consumed\ (Wh)}{Total\ distance\ travelled\ (km)}$

For ease of use, range for the vehicle is equals to

$$\frac{18360}{\frac{Wh}{km}\ value} \ (km).$$

### 3. RESULT AND ANALYSIS

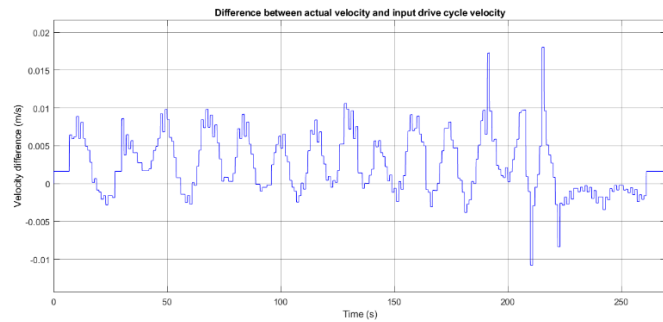
The electric converted vehicle was tested on the road and experimental data were obtained for analysis and comparison purpose. Battery pack current, battery pack voltage, motor current, motor torque, motor speed, vehicle speed, and battery pack SOC data were obtained from the vehicle monitoring software.

Fig-9: Speed profile from experimental data



The cell data are extracted from [17] [22] for genericbattery modeling method.

A PD controller is employed in the model to regulate the reference and actual vehicle speed in a closed loop. Reference speed and actual speed of the vehicle differed negligibly showing that the PD controller worked well as shown in figure 10.



**Fig-10:** Maximum speed error values graph

The energy consumption ratio of the experimental data is 251.5, whereas it is 113.2 in the simulated mode, for a transmission efficiency of 85%. The high value of the energy consumption ratio in the experiment was due to losses present in the old transmission system. The energy consumption value fluctuates at first; however, it attains a constant value over time as shown in figure 11.

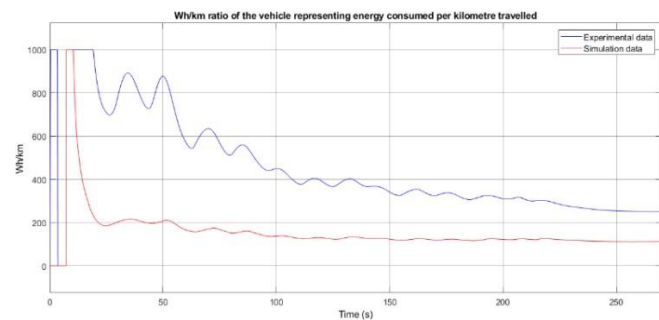


**Fig-11:** Energy consumption ratio graph

The starting torque value of the motor in the simulated model is 115 Nm whereas the torque reached 180 Nm during the experiment as shown in figure 12. One of the reasons could be due to insufficient gear ratio (i.e. 3.5:1) in the transmission system of the vehicle. The optimal gear ratio for the system is approx. 8:1 as per the model. This could have caused the motor to draw a high current from the controller during the start of the vehicle.

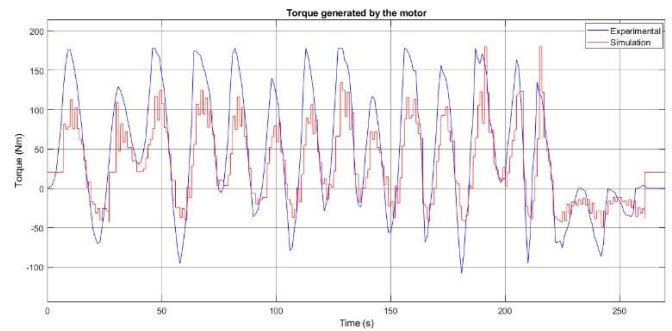


**Fig-12:** Motor torque graph

The terminal voltage data of the battery had fluctuations in the experiment as shown in figure 13. The value dropped to about 105 V but recovered to the original value quickly. However, the voltage constantly dropped to 106 V and didn't recover to the original value in the simulated data. The generic battery model couldn't be as accurate as the actual equivalent circuit battery model which accounted for time constants for the battery, resulting in an error in the prediction of open circuit voltage.

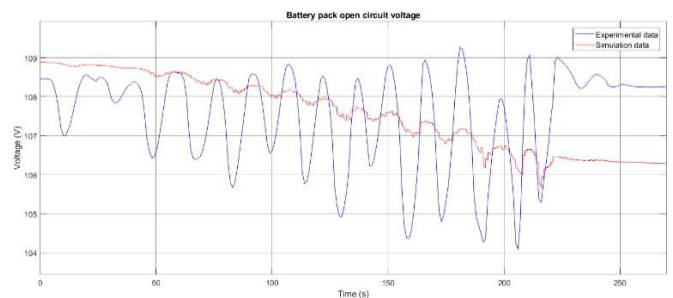


**Fig-13:** Battery OCV graph

There was a slight difference in battery current drawn between the simulated and experimental data. The difference could be due to ill configuration of the motor or inefficiencies present in the model configuration. The battery model could also affect the current value. The battery current value in the experimental data was higher than the simulated value as shown in figure 14.

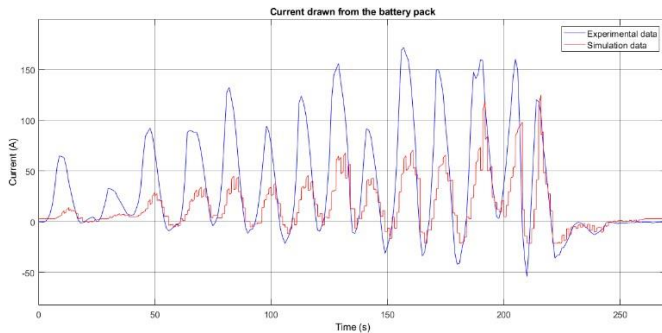


Fig-14: Battery current graph

In the experimental data, SOC didn't drop whereas, in the simulated model, it dropped from 98% to almost 97% as shown in figure 15. The error could be due to the least count of the SOC meter in the experiment. Furthermore, the generic battery model could have affected the SOC which couldn't exhibit the accurate behavior of the battery pack used in the vehicle.

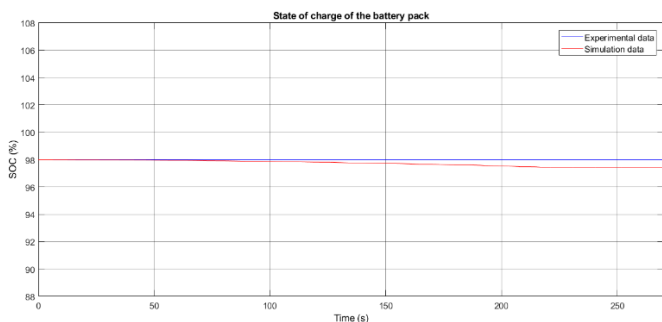


Fig-15: Battery pack SOC graph

#### 4. CONCLUSION

The overall model is working efficiently. The discrepancy in the starting motor torque is largely due to the insufficient gear ratio and the unaccounted losses in the model. In addition to what is already done, if other pieces of information about the motor and controller parameters are received from the manufacturer, the model would be more efficacious. Also, the battery model should be accurate and efficient to get the actual SOC graph. Conclusively, the model can be used at the design stage in similar EV conversion projects to determine the equipment specifications and carry out performance analysis of the vehicle.

#### 5. ACKNOWLEDGEMENT

This project was funded by the Young Scientist Encouragement Fund, Ministry Of Social Development, Bagmati Province, Nepal. The sum of NRs. 20 lakhs (~ 20 thousand dollars) was awarded for the development and testing of a prototype electric converted vehicle. The

improvement of the prototype continues as an ongoing research project.

#### 6. REFERENCES

- [1] S. Paudel, G. Raj Pokharel, N. Bhattarai, and S. Shrestha, "Evaluating the Effect of Policies, Vehicle Attributes and Charging Infrastructure on Electric Vehicles Diffusion in Kathmandu Valley of Nepal".
- [2] M. Crippa et al., "GHG emissions of all world countries 2021 Report." doi: 10.2760/173513.
- [3] S. Kaleg, A. Hapid, and M. Kurniasih, "Electric Vehicle Conversion Based on Distance, Speed and Cost Requirements," *Energy Procedia*, vol. 68, pp. 446–454, Apr. 2015, doi: 10.1016/j.egypro.2015.03.276.
- [4] A. Ukaew, "Model Based System Design for Electric Vehicle Conversion," in *New Trends in Electrical Vehicle Powertrains*, IntechOpen, 2019. doi: 10.5772/intechopen.77265.
- [5] "Worldwide Harmonized Light Vehicles Test Cycle (WLTC)," DieselNet. <https://dieselnet.com/standards/cycles/wltp.php>.
- [6] I. Miri, A. Fotouhi, and N. Ewin, "Electric vehicle energy consumption modeling and estimation—A case study," *International Journal of Energy Research*, vol. 45, no. 1, pp. 501–520, Jan. 2021, doi: 10.1002/er.5700.
- [7] K. N. Genikomsakis and G. Mitrentsis, "A computationally efficient simulation model for estimating energy consumption of electric vehicles in the context of route planning applications," *Transportation Research Part D: Transport and Environment*, vol. 50, pp. 98–118, Jan. 2017, doi: 10.1016/j.trd.2016.10.014.
- [8] C. Sunanda, "Modeling and Performance Analysis of an Electric Vehicle with MATLAB/Simulink," *International Research Journal of Engineering and Technology*, p. 1098, 2008, [Online]. Available: [www.irjet.net](http://www.irjet.net).
- [9] S. Chauhan, "Motor Torque Calculations for Electric Vehicle," *International Journal of Scientific & Technology Research*, vol. 4, p. 8, 2015, [Online]. Available: [www.ijstr.org](http://www.ijstr.org).
- [10] M. Ehsani, Y. Gao, S. E. Gay, and A. Emadi, "Modern Electric, Hybrid Electric, and Fuel Cell Vehicles: Fundamentals, Theory, and Design".

- [11] J. Wang, I. Besselink, and H. Nijmeijer, "Battery electric vehicle energy consumption prediction for a trip based on route information," Proceedings of the Institution of Mechanical Engineers, Part D: Journal of Automobile Engineering, vol. 232, no. 11. SAGE Publications Ltd, pp. 1528–1542, Sep. 01, 2018. doi: 10.1177/0954407017729938.
- [12] L. Jeongwoo and D. J. Nelson, "Rotating inertia impact on propulsion and regenerative braking for electric motor driven vehicles," *2005 IEEE Vehicle Power and Propulsion Conference, VPPC*, vol. 2005, pp.308–314, 2005, doi: 10.1109/VPPC.2005.1554575.
- [13] K. Warake, S. R. Bhahulikar, and N. v Satpute, "Design & Development of Regenerative Braking System at Rear Axle," 2018. [Online]. Available: <http://www.ripublication.com>.
- [14] Sandeep, V., Shastri, S., Sardar, A., & Salkuti, S. R. (2020). Modeling of battery pack sizing for electric vehicles. *International Journal of Power Electronics and Drive Systems (IJPEDS)*, 11(4), 1987. doi:10.11591.ijpeds.v11.i4.pp1987-1994.
- [15] Fotouhi, A., Auger, D. J., Propp, K., Longo, S., & Wild, M. (2016). A review on electric vehicle battery modelling: From Lithium-ion toward Lithium-Sulphur. *Renewable and Sustainable Energy Reviews*, 56, 1008–1021, doi:10.1016/j.rser.2015.12.009.
- [16] Saldaña, G., San Martín, J. I., Zamora, I., Asensio, F. J., & Oñederra, O. (2019). Analysis of the Current Electric Battery Models for Electric Vehicle Simulation. *Energies*, 12(14), 2750, doi:10.3390.en12142750.
- [17] Yao, L. W., Aziz, J. A., Kong, P. Y., & Idris, N. R. N. (2013). Modeling of lithium-ion battery using MATLAB/Simulink. *IECON 2013 - 39th Annual Conference of the IEEE Industrial Electronics Society*, 1729-1734, doi:10.1109/IECON.2013.6699393.
- [18] Miri, I., Fotouhi, A., & Ewin, N. (2020). Electric vehicle energy consumption modelling and estimation -A case study. *International Journal of Energy Research*, 45(1), 501–520, doi:10.1002.er.5700.
- [19] Yu, Y., Narayan, N., Vega-Garita, V., Popovic-Gerber, J., Qin, Z., Wagemaker, M., Bauer, P., & Zeman, M. (2018). Constructing Accurate Equivalent Electrical Circuit Models of Lithium Iron Phosphate and Lead-Acid Battery Cells for Solar Home System Applications. *Energies*, 11(9), 2305, doi:10.3390.n11092305.
- [20] Su, J., Lin, M., Wang, S., Li, J., Coffie-Ken, J., & Xie, F. (2019). An equivalent circuit model analysis for the lithium-ion battery pack in pure electric vehicles. *Measurement and Control*, 52(3–4), 193–201, doi: 10.1177.0020294019827338.
- [21] "Effect of Different Regenerative Braking Strategies on Braking Performance and Fuel Economy in a Hybrid Electric Bus Employing CRUISE Vehicle Simulation," 2008.
- [22] Tremblay, O.; Dessaint, L.-A. (2009). Experimental Validation of a Battery Dynamic Model for EV Applications. *World Electric Vehicle Journal*, 3 (289-298), doi:10.3390.wevj3020289